water

Article

A GIS-Based Flooding Indicator for Heavy Rainfall Hazards Along the German Railway Network: Case Study Nordrhein-Westfalen

Frauke von den Driesch * and Sonja Szymczak

German Centre for Rail Traffic Research at the Federal Railway Authority (DZSF), 01219 Dresden, Germany; szymczaks@dzsf.bund.de
* Correspondence: vondendrieschf@dzsf.bund.de

Abstract

Climate-induced natural hazards can result in disruptions and failures of railway routes which are associated with high economic costs. Hence, the mechanisms of climate impacts posing a threat to rail transport must be identified, analysed and localised in railway networks. This study aims at assessing heavy rainfall hazards on the railway network of the federal state Nordrhein-Westfalen (NRW) in Germany and presents a GIS-based flooding indicator. A rule-based classification and aggregation approach with a hazard matrix was developed using potential flooding depths and flow velocities, resulting in five hazard classes. The approach was applied to the railway network in NRW for two heavy rainfall scenarios (N_{100}, N_{ext}). The results show that the clear majority of route kilometres are classified as at least moderate hazard in both precipitation scenarios considered (N_{ext} 81%, N_{100} 72%). On railway routes in low mountain range regions, more sections are assigned higher hazard classes than in flat landscapes. The plausibility of the indicator was explored through scenario, structural and conceptual parameter analyses, which support robustness of the results. The maps can serve as a tool for making qualitative statements on the potential impact on the German railway network and localising these impacts spatially.

Keywords: railway; flooding; heavy rainfall; natural hazard assessment; exposure analysis; hazard indication maps; GIS

Academic Editors: Oluwafemi E. Adeyeri and Kazeem Abiodun Ishola

Received: 3 February 2026
Revised: 12 June 2026
Accepted: 18 June 2026
Published: 23 June 2026

1. Introduction

Adaptation to climate change is essential for a functioning and efficient railway system, as railways are an essential part of the European transport system. Railway transport plays an important role in the European economy by supplying goods and services on a large scale [1–3]. As of 2023, the German railway network covers more than 39,000 km of routes and has the highest passenger numbers and the highest volume of goods (in tons) transported in the European Union [4–6].

Extreme climatic events such as heavy rainfall, droughts or storms can lead to flooding, fires and tree falls, which in turn can have large impacts on the railway infrastructure and rolling stock [3,7]. Heavy rainfall events can cause extensive widespread flooding and are associated with being potential triggers for other natural hazards, such as gravitational mass movements and river floods [8–11]. For example, the heavy rainfall events in July 2021 in western Germany and adjacent countries led to extreme floods resulting in landslides, embankment slides and track undermining and overwashing with damage to all parts of the railway infrastructure [8,10,11]. Disruptions and failures of railway routes are associated with high economic costs [3,12]. Deutsche Bahn, Germany's largest railway operator, estimates the related direct damage to their infrastructure from the July 2021 heavy rainfall and flood event at around € 1.3 billion. Some railway lines were completely destroyed and the restoration took several years [13,14]. Route closures, diversions and damage to infrastructure components have also occurred in connection with other heavy rainfall events in Germany in the past, e.g., in Münster in 2014, and in both Kitzingen and in Schwäbisch Gmünd in 2024 [15–17].

Among other natural hazards, heavy-rainfall-induced flooding poses a particular threat to railway infrastructure as it can occur in a spatially diffuse manner and is characterised by both potentially large volumes of water with high flow velocities and a high erosion potential [8,18,19]. A spatio-temporal analysis compared damage data from Deutsche Bahn with the heavy rainfall event catalogue "CatRaRe" (Catalogue of Radar-based heavy Rainfall Events in Germany) of the German Weather Service (DWD) and showed that between 2011 and 2021 nearly all parts of the German railway network were affected at least once by a heavy rainfall event [11]. Given these historical occurrences and damages, as well as the expected increase in extreme events with climate change in Germany [20], it is essential to localise and classify the hazards of flooding caused by heavy rainfall in the German railway network. Therefore, this study addresses this gap by providing an initial indicative GIS-based method to identify potential focal points and areas of exposure within the railway network.

GIS-based analyses and hazard maps are an important tool for the spatial assessment of climate impacts on infrastructure and are frequently used in the transport sector. Some studies investigate multiple natural hazards or analyse a basic influence of climate impacts or climate change [21–23]. Within GIS-based studies on the spatial assessment of climate impacts on transport infrastructure, there are only a few investigations focusing specifically on railway infrastructure, most of them focussing on other climate impacts than flooding [24–29]. These studies refer to different networks, e.g., the Czech railway network [24], the Spanish railway network [25], the German road network [26,27] and the German railway network [28,29], and different natural hazards or impacts, e.g., rapid mass movements [28], embankment fires or wild fires [25,29], and tree-fall events [24,29]. Whilst hazard indication maps already exist for multiple hazards in the German railway network and are used in research and practice [30], there is a clear gap in this area with regard to heavy rainfall hazards, which is addressed in the study presented here, building directly on established methodologies.

Existing GIS-based approaches on the flooding of railway infrastructure mainly aim at identifying hotspots of flooding hazards against the background of climate change on specific railway lines [31–33] or on whole railway networks [34–36]. Only a few studies worked on approaches to heavy rainfall impact assessment on railway infrastructure. Fabella & Szymczak and Liu et al. used geodata investigating heavy-rainfall-induced hazards, e.g., landslides, on railway infrastructure but with a main focus on statistical correlations between heavy rainfall and other processes and parameters [7,36]. Some studies conducted comprehensive multi-criteria assessments addressing flooding risks on railways using complex methodological frameworks and a wide variety of input data [37–39]. In contrast to such multi-criteria assessments, this study presents a less complex approach focussing on exposure and hazard analysis by considering two parameters, flooding depth and flow velocity. This study makes use of existing high-resolution heavy-rainfall modelling data for Germany, which already takes various geographical parameters into account, such as terrain elevation, precipitation scenarios, and land use [40,41]. These maps provide spatially comprehensive data on flooding depths and flow velocities, but there is no methodology available to derive hazards specifically on the railway network from these data. To address this gap, this study design is specifically chosen to ensure

https://doi.org/10.3390/w18131533

that the approach can easily be replicated and further developed utilising high-quality input data that is already available. Consequently, the methodology can serve as a starting point for further, more complex investigations and be applied in such contexts, such as comprehensive risk analyses including sensitivity and criticality factors. However, these complex investigations are beyond the scope of the current study.

Several studies focus on river-flooding-induced damages of railway infrastructure and explanatory parameters, e.g., flooding depths. Kellermann et al. analysed occurred damages on the railway infrastructure after the March river flooding event 2006 in Austria and developed a model for estimating flood losses in railway infrastructure based on different explanatory parameters [42]. While Zhu et al. investigated the effects of river flooding on the operability of railway systems in China using a simulation framework, Tsubaki et al. developed fragility curves for the risks of different structural damages to railway infrastructure in case of river flooding [43,44]. Unlike those studies, our study does not focus on concrete damage analysis or estimation. Instead, it uses the findings from such damage study procedures to develop and apply a classification approach on potential hazards to the German railway network on an indicative level.

Our study presents an exposure and hazard analysis of railways to heavy rainfall. This needs to be carried out as a contribution to adapting the railway infrastructure in the long term. Exposure analyses in already existing and successfully applied guidelines for municipal heavy rainfall risk management in Germany take modelled flooding depths and flow velocities into account, as well as using hazard classes based on potential damage due to physical forces [45,46]. The physical forces of flowing water can also lead to damage processes affecting the railway infrastructure, e.g., erosion or deposition of debris. While these guidelines do not analyse the exposure and hazard of transport infrastructure specifically and only cover limited areas, the approach in this paper aims at providing a tool for analysis of railways indicating exposure and hazards on network and route level.

This study presents a GIS-based flooding indicator as an initial approach to assess heavy-rainfall hazards on the German railway infrastructure. It aims at providing an easily replicable tool for indicative exposure and hazard analyses in the German railway network. The following research questions are addressed:

- How can a potential heavy-rainfall hazard on the German railway network be derived spatially as an indicator on the basis of existing heavy-rainfall hazard indication maps?
- How can the derived heavy-rainfall hazards on the German railway network be visualised spatially along the railway routes?
- What potential heavy-rainfall hazards can be derived for the railway network in Nordrhein-Westfalen and are there regional patterns?

In order to address the research questions and achieve the study's objective, a rule-based hazard classification is conducted based on parameters, classifications and thresholds from the literature and using already available high-quality input data. As a first step, an indicative classification approach to assessing the potential exposure of railways to heavy rainfall is developed based on flooding depths and flow velocities including spatial aggregation along the railways. In a second step, this approach is applied to the railway network of the federal state of Nordrhein-Westfalen (NRW) in Western Germany to get spatial information on potential exposure to heavy rainfall impacts. To explore the robustness and plausibility of the methodology and resulting GIS-based hazard maps, some supplementary analyses were conducted in a third step. These include varying input data, classification schemes and parameters as well as regional differentiation of the resulting flooding indicator.

2. Materials and Methods

2.1. Study Area and Input Data

This study focuses on the railway network in NRW, a federal state located in Western Germany (Figure 1a). NRW is the fourth largest federal state in terms of area and the largest federal state in terms of population with the second largest railway network density in Germany (14% of the whole German railway network is located in NRW) (Figure 1b). Two important European rail freight corridors cross NRW (Rhine–Alpine and North Sea–Baltic), and two of the 10 most important stations in terms of passenger volume (central station Köln Hbf and Düsseldorf Hbf) are located in this federal state [47,48]. As a result, disruptions in NRW often have an impact on the entire German railway network. The state's railway network experienced a high impact of heavy rainfall events in the past, notably in 2021 [9,10]. Therefore, NRW was selected as a suitable study area to develop the flooding-indicator approach.

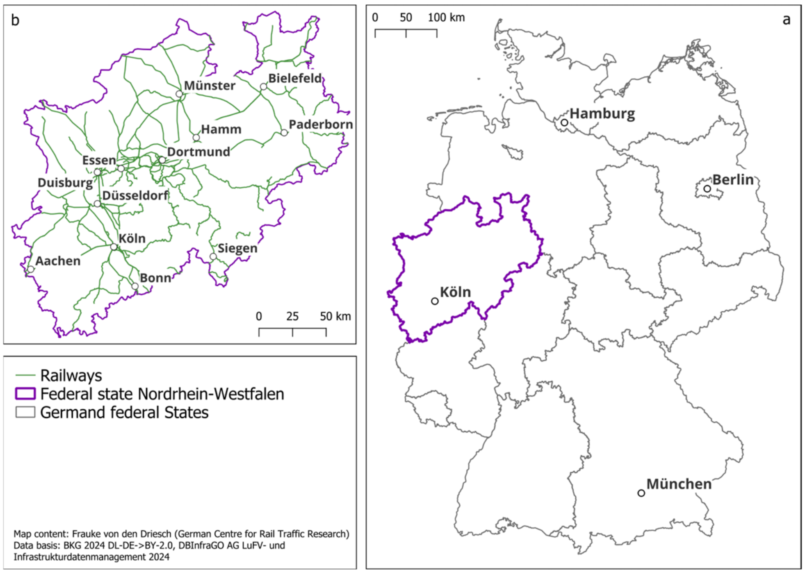

Figure 1. (**a**) Location of the study area in Germany and (**b**) overview of the study area federal state Nordrhein-Westfalen (NRW).

For the development of the flooding indicator, the railway network and heavy-rainfall hazard indication maps were needed as input data. The nationwide German railway network from Deutsche Bahn is freely available as polyline vector data [49]. The latest version available at the time of GIS analysis (updated in 2024) was used in this study. The data set includes the railway routes as single-line features with several appending information per route, e.g., number of tracks, route number or electrification. It is important to notice that both single-track and double-track routes are represented with only one line per route.

The entire railway network from Deutsche Bahn in Germany comprises approximately 33,900 km of routes. As this study focuses on NRW, the data set was cropped to the extents of the federal state resulting in a total of approximately 4800 km of routes (Figure 1b).

Under the leadership of the German Federal Agency for Cartography and Geodesy (BKG) several federal and state authorities are currently developing a Germany-wide indication map on heavy rainfall hazards [40]. With this project, the BKG is aiming for a standardised and comprehensive mapping of heavy rainfall hazards in Germany. The maps are to be understood at an indicative level and can form a basis for detailed analyses, to develop specific local measures, for example.

As a pilot project, the maps were created based on 2D-hydrodynamic modelling for the federal state of NRW and published in 2021 as a map product and as raster datasets of flooding depth and flow velocities [41]. The 2D-hydrodynamic modelling incorporates various data, e.g., digital terrain models, land-use data, heavy-rainfall statistics and culvert data. Model simulations for NRW were carried out for two different precipitation scenarios: (1) a 100-year event (N_{100}) based on the KOSTRA-DWD-2010R data set (heavy rainfall statistics) of the German Weather Service (DWD), and (2) an extreme event (N_{ext}), which was calculated with a fixed precipitation intensity of 90 mm per hour for one hour of simulated rainfall. These precipitation scenarios can be categorised as intense and extreme events using the heavy-rainfall index developed by Schmitt [50,51], which classifies the severity of heavy-rainfall events based on their return period and is commonly used in hazard and risk communication in Germany [52]. As a result of the modelling, hazard indication maps for NRW are available as raster data sets of the modelled flow velocities and flooding depths for each precipitation scenario. The raster data of the flow velocities include the values of the magnitude, while values for the flow direction were not available at the time of the GIS analysis. Flow velocity values are given in metres per second (m/s), and the flooding depths in metres (m). The raster data is provided as 10 km × 10 km tiles with a 1 m × 1 m resolution (one value per square metre) [41].

2.2. Development and Application of Flooding Indicator

A rule-based classification and aggregation approach was chosen to provide an easily replicable tool for indicative heavy rainfall exposure and hazard analyses in the German railway network. It is based on parameters, classification approaches and thresholds from the literature. An in-depth analysis of the July 2021 event in Germany along a railway route section found that most flood-induced damages affected the track superstructure, surrounding areas, track substructure and technical infrastructure while the most frequently identified damage processes were erosion and debris transport or deposit [11]. As these damage patterns and processes are strongly related to the flooding depths and flow velocities occurred [11,42,44,53], the study presented focussed on a classification approach combining these two parameters. The determination of classes and class boundaries for water depth and flow velocities was founded on a literature-based methodology that takes both qualitative and quantitative studies and guidelines into account. These sources serve as the basis for the classification scheme, in which the findings from the literature were adapted in order to determine hazard of German railways to heavy rainfall induced flooding.

While several concepts for general damage functions for river flooding events on railway infrastructures exist, only a few studies developed and validated concrete threshold values (depth and velocity) and classifications for direct structural damages [54–57]. Flooding depth threshold values for operability of railways were set by Zhu et al. (0.2 m) and Murdock et al. (0.1 m) [43,58]. These studies use flooding depths as an indicator for system functionality and do not focus on direct structural damages of railway infrastructure components. Schriewer et al. compared sites of structural damages of railway infrastructure spatially to heavy rainfall indication maps from BKG as well as river flood hazard maps [11]. The study showed that damage occurs in all water depth classes considered, even in areas with very shallow water depths (<0.1 m), especially when the heavy rainfall indication maps are considered. Kellermann et al. modelled the March river flooding event in spring 2006 in Austria and analysed flooding depths in relation to the actual damages that occurred [42]. They then developed three structural damage classes for railway infrastructure, which are ordinal-scaled by damage progression and refer to standard cross-sections consisting of the components substructure, superstructure, catenary and signals.

Based on statistical analyses, they also determined threshold values of flooding depths for the damage classes. River flooding and heavy-rainfall-induced flooding can result in similar, though not identical, damage mechanisms to railway infrastructure. Therefore, the classes and threshold values for flooding depth by Kellermann et al. were used in the development of the flooding indicator in this study, as Schriewer et al. did not set concrete threshold values for water depth for the presented damage classes (Table 1) [11,42].

Table 1. Depth classes based on their potential impacts to railway infrastructure (data basis: [42]).

Class	Flooding Depth (m)	Expected Structural Damage [42]	Definition for Flooding-Indicator Development
1	<0.2	"Track's superstructure is partly impounded, but there is no or only little noticeable damage".	No or minor damages to individual railway infrastructure components can be expected.
2	0.2–1.4	"Substructure und superstructure of the track section are fully inundated and significant structural damage at least to the substructure must be expected".	Significant damages to several railway infrastructure components can be expected.
3	>1.4	"Additional damage to the superstructure, catenary and/or signals must be expected and, most commonly, the standard cross-section of the affected track section needs to be completely restored".	Severe damages to several railway infrastructure components or destruction of sections can be expected.

Based on the indicated importance of flow velocity in several studies, flow velocity was selected as the second parameter in our classification approach [37,42,53,59]. Although these studies highlight the importance of flow velocity as an indicator for potential damage, there is still a need to develop concrete threshold values and classification of flow velocity. Following the qualitative literature-based methodology in this study, velocity classes from exposure and hazard analyses in existing guidelines for municipal heavy-rainfall risk management in Germany were used [45] (Table 2). MULNV NRW categorises flow velocities into three classes based on their potential hazards to human health, infrastructure (power supply, telecommunication, transport) and objects (buildings), e.g., hazards to people with restricted mobility and children, potential wall failure and potential failure of structural elements [45]. An increased potential hazard is assumed for flow velocities from 0.2 m/s as a critical value. As the presented study aims to assess the exposure and hazard to railway infrastructure and its potential structural damages, it is assumed that the physical forces leading to damages on structural components of buildings and diverse infrastructures can also lead to structural damages of railway infrastructure. Therefore, the class boundaries from the guideline were adopted and the classes were defined for flooding-indicator development (Table 2). While class 1 with <0.2 m/s is considered with no increased hazard in municipal heavy rainfall risk management [45], the definition for class 1 in this study takes the possibility of minor damages into account.

https://doi.org/10.3390/w18131533

Table 2. Velocity classes based on their potential impacts to infrastructure and objects (data basis: [45]).

Class	Flow Velocity (m/s)	Potential Hazards [45]	Definition for Flooding-Indicator Development
1	<0.2	No increased hazard.	No damage or minor damages to individual railway infrastructure components can be expected.
2	0.2–0.5	Failure of seals due to increased pressure, e.g., door seals.	Minor or moderate damages to individual or several railway infrastructure components can be expected.
3	0.5–2.0	Possible breakage of walls due to a combination of high static and dynamic compressive forces.	Significant damages to several railway infrastructure components can be expected.
4	>2.0	Possible failure of structural components due to increased dynamic compressive forces. Possible failure of structural components due to entrained solids. Damage to the structure due to undermining.	Severe damages to several railway infrastructure components or destruction of sections can be expected

In the next step, the classified flooding depths and flow velocities were combined in a hazard matrix to derive a flooding indicator, which comprises four hazard classes (Table 3). A similar approach for municipal infrastructures exists in the exposure and hazard analyses guidelines for municipal heavy rainfall risk management in Baden-Württemberg (BW), Germany [46]. In order to optimise this approach to railway infrastructure, a hazard matrix was developed by combining classified flooding depths and flow velocities with class boundaries as described above. The combination of classified flooding depths and flow velocities results in a classified flooding indicator as shown in Table 3. The four resulting classes of the classified flooding indicator are labelled as low, moderate, high and very high hazard. Combinations of different input classes, e.g., flooding depth class 2 and flow velocity class 1, result in a flooding indicator of the respective higher class. All combinations with highest class flow velocities or highest class flooding depths are categorised as very high in the flooding-indicator class.

Table 3. Hazard matrix combining the flooding depths and flow velocities to derive a classified flooding indicator.

		Maximum Flooding Depth (m)		
		<0.2	0.2–1.4	>1.4
Maximum flow velocity (m/s)	<0.2	low	moderate	very high
	0.2–0.5	moderate	high	very high
	0.5–2.0	high	very high	very high
	>2.0	very high	very high	very high

The technical implementation of the methodology was carried out in Python code using QGIS functionalities. A script-based application was chosen to ensure the traceability, reproducibility and replicability of the methodology. On the one hand, this makes it possible in principle to further develop the method in a comprehensible manner and, on the other hand, to transfer the method to other regions and other land-based modes of transport. The processing of the geodata was carried out entirely with the functionalities of the qgis.core module, which includes SAGA GIS and GRASS GIS functions in addition to QGIS functions (QGIS version 3.28 with Python version 3.9).

The flooding depth and flow velocity data from the extreme precipitation scenario were used here. First, the raster data for depth and velocity in the selected tile were matched for further processing in order to minimise the processing time in the subsequent processing steps as well as the resulting data products. Therefore, the raster data was cropped to an area of interest within a 10 m buffer distance at each side around the given railway routes to counteract a potential inaccuracy in the position of the tracks in relation to the route polylines in the vector data set and to take into account railway infrastructure components next to the tracks in the analysis.

Then, the classification method was applied on the cropped raster data on water depth and flow velocities by classifying the raster values based on the classes in Table 2 in a first step, resulting in separate classified rasters for water depth and flow velocity with a class value for each 1 m × 1 m raster cell (Figure 2).

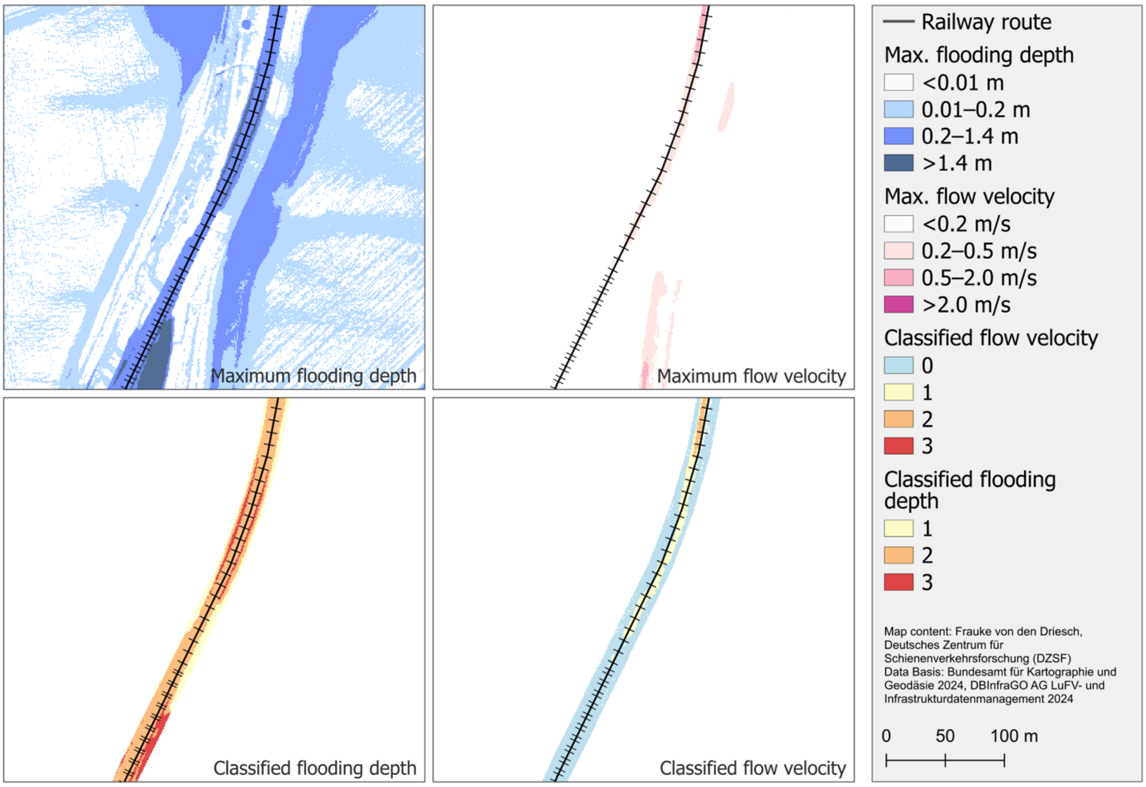

Figure 2. Classified rasters for water depth and flow velocity based on maximum flooding depth and maximum flow velocities (N_{ext}).

Following the developed hazard matrix, the classified depth and velocity rasters were combined to derive a flooding indicator, which comprises four hazard classes: low, moderate, high and very high. The result is a raster with one indicator class per 1 m × 1 m raster cell for the area of interest, i.e., within a 10 m buffer distance around the railway lines (Figure 3).

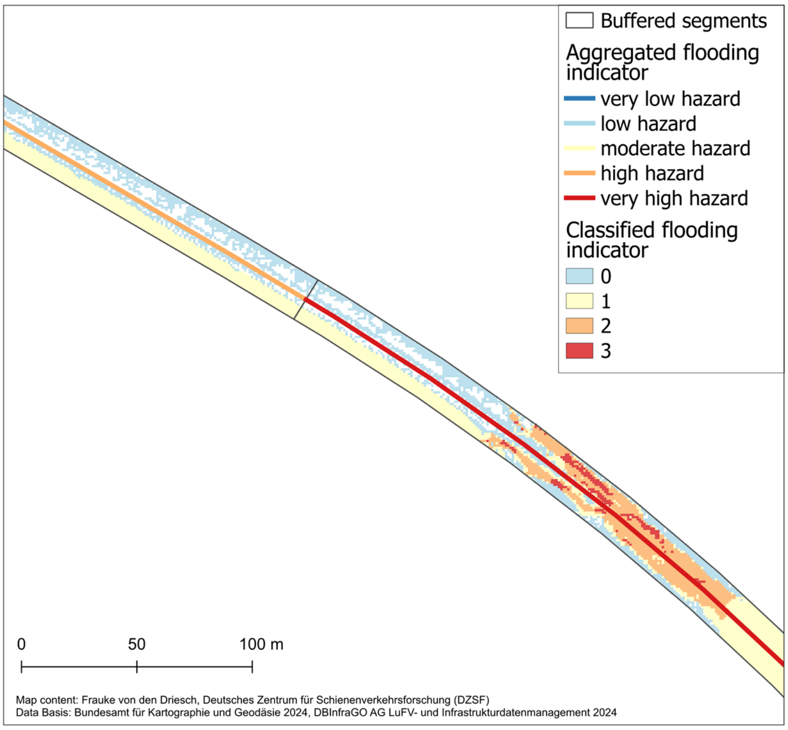

Figure 3. Raster-based classified flooding indicator and vector-based spatially aggregated flooding indicator (N_{ext}).

To derive information on exposure to heavy rainfall impacts for each route, the flooding-indicator information was transferred from gridded data to linear data of the railway network. For this purpose, a method for the spatial aggregation of the raster data was developed, which takes the maximum class value, the mean class value and the proportion of flooded area into account.

For this purpose, the railway routes were divided into segments of equal size (500 m) and then buffered (10 m). For each buffer polygon, zonal statistics were derived from the classified flooding-indicator rasters, comprising mean class values, maximum class values and number of classified raster cells (Figure 3). The number of classified raster cells was divided by the total number of raster cells in the polygon to derive the proportion of flooded area. The flooded area share was classified to derive an area factor for further calculation (Table 4).

Table 4. Area factor as classified flooded area share.

Area Share	Area Factor
<25%	0.25
25–50%	0.5
50–75%	0.75
>75%	1.0

The spatial aggregation of the flooding indicator was performed by multiplying the mean class value, maximum class value and area factor for each segment. The multiplication product was rounded to whole numbers, which is the final aggregated flooding-indicator class according to Table 5. Areas without modelled or with extremely low flooding depths and/or flow velocities were not assigned an indicator class based on the described methodology. However, a potential impact in the event of a heavy rainfall event cannot be completely ruled out on the basis of the modelled results. Additionally, the findings from Schriewer et al. emphasise that structural damages to railway infrastructure can likely occur in areas with very low flooding depths according to hazard maps [11]. Therefore, a fifth indicator class very low hazard was added to include areas where there are no or only extremely low modelled flow velocities and/or flooding depths (Table 5). The final geodata product is a polyline vector layer with an assigned flooding indicator class for each line segment.

Table 5. Aggregated flooding indicator class based on rounded multiplication product of mean class value, maximum class value and area factor.

Class	Product
very low	NULL
low	0
moderate	1
high	2
very high	≥3

2.3. Exploratory Plausibility Analyses

In order to investigate the plausibility of the approach developed in this study as well as the resulting flooding indicator, some supplementary analyses were conducted including variations in input scenarios, classification scheme structure and input parameters as well as a spatial differentiation of the results. As the chosen methodology is a qualitative rule-based hazard classification and no empirical calibration is carried out, the analyses conducted are considered as exploratory investigations into the robustness and plausibility of the methodology and resulting heavy-rainfall hazard patterns for railways. The calculation run following the methodology as described in Section 2.2 served as base run A for the following analyses, unless stated otherwise.

Firstly, a regional differentiation analysis was carried out to explore spatial differences in resulting heavy rainfall hazards throughout the railway network in NRW. To explore regional differences related to the state's diverse topography, the results of base run A were analysed for four large natural areas, which are based on geological history: Westfälische Bucht (WFB), Rheinisches Schiefergebirge (RSG), Niederrheinische Bucht und Tiefland (NBT) and Weserbergland (WBL). While WFB and NBT are characterised by relatively flat topography, RSG and WBL are classified as low mountain ranges [60].

In the second step, a scenario analysis was conducted to explore the reaction to different input scenarios. In addition to base run A, which used an extreme precipitation scenario (N_{ext}) as input, the methodology was applied to the railway network in NRW using the second available precipitation scenario data set with water depths and flow velocities for NRW, a 100-year scenario (N_{100}) (run B).

In the third step, a structural analysis was carried out to investigate the influence of the classification decision for water depths. Therefore, an additional calculation run was carried out using the classification scheme from the exposure and hazard analyses in the guideline for municipal heavy rainfall risk management in NRW, which is shown in Table 6 [45] (run C). The water depth impact classes from the guideline were not specifically developed for railway infrastructure. Nevertheless, the physical forces considered there can possibly lead to structural damages of railway infrastructure, which is why it was used here as a comparison. Compared to the classification scheme in base run A (Table 1), the classification scheme in run C comprises four classes instead of three with consequently different class boundaries (Table 6). Consequently, the hazard matrix (Table 7) is also slightly different from the hazard matrix in base run A (Table 3). Spatial aggregation was performed identically for both calculation runs as described in Section 2.3 resulting in five aggregated flooding-indicator classes, which enabled comparability of the results.

Table 6. Depth classes based on their potential impacts to objects and infrastructure (data basis: [45]).

Class	Flooding Depth (m)	Potential Hazards [45]
1	<0.1	No increased hazard.
2	0.1–0.5	Water ingress into objects at ground level and below, e.g., parts of buildings.
3	0.5–1.0	Water ingress into objects above ground level. Danger to public infrastructure facilities, e.g., electricity, telecommunications.
4	>1.0	Possible failure of structural components.

Table 7. Hazard matrix combining the flooding depths and flow velocities to derive a classified flooding indicator in calculation run C.

		Maximum Flooding Depth (m)			
		<0.1	0.1–0.5	0.5–1.0	>1.0
Maximum flow velocity (m/s)	<0.2	low	moderate	moderate	very high
	0.2–0.5	moderate	moderate	high	very high
	0.5–2.0	moderate	high	very high	very high
	>2.0	very high	very high	very high	very high

In the fourth step, a conceptual parameter analysis was carried out to investigate the relative influence of the input parameters water depth and flow velocity on the resulting heavy rainfall hazards on the railway network. For the parameter analysis, a classification scheme with the same number of classes for both water depth and flow velocity was needed, which is not given in the previously used base run A (Tables 1 and 2). Therefore, the additional calculation run from the structural analysis was chosen as the base run here (run C). For run C, the classification schemes from the exposure and hazard analyses in the municipal heavy rainfall risk management guideline were used, which comprised four classes for both water depth and flow velocity [45] (Tables 2 and 6). In addition to base run C, two runs of the indicator methodology were conducted with either water depth (run D1) or flow velocity (run D2) as the sole parameter in the classification scheme. Consequently, no combination of the two parameters in a hazard matrix was carried out in these runs and only the chosen parameter contributed to indicator classification.

In a fifth step, a local case study was performed to explore the plausibility of the results of this study against a past flooding event. For the precipitation, runoff and river discharge associated with the flooding event in July 2021 in western Germany, return periods of well over 100 years were adopted across large parts of the affected regions [61,62]. Therefore, the results of base run A were used, which used an extreme precipitation scenario as the input. During the July 2021 heavy rainfall and flooding event, many railway routes were damaged and partly destroyed [10,11]. A damage analysis study on a section of the railway route 2631 between the train stations Kall and Nettersheim in NRW mapped some of the most frequent damage processes occurred [11]. The route section under consideration is situated in the Eifel low mountain range, which is part of the natural landscape RSG. As the underlying geodata was not available, the damages were georeferenced in QGIS on the basis of the publication [11]. The mapped damages were compared with the flooding-indicator hazard classes for this route section.

3. Results

3.1. Indicated Heavy Rainfall Hazards for the Railway Network in NRW

The application of the flooding-indicator methodology to the railway network in NRW resulted in (1) detailed and (2) aggregated maps of the heavy rainfall hazard per scenario N_{100} and N_{ext} for the railway network in NRW (Figure 4). The detailed maps show a grid-based flooding indicator with one value per square metre in an area of 10 m buffer width around the routes. The detailed flooding indicator in these maps is shown in the four classes low, moderate, high and very high hazard, according to the class formation described in the methods (Section 2.2). The aggregated maps show the determined flooding indicator as vector-based polyline data with a value for each route section, which is usually 500 metres long (Figure 4a,b). However, at the start and end of the route and at tile boundaries, the sections may be shorter due to processing. We show the aggregated flooding indicator in these maps in five classes: very low, low, moderate, high and very high hazard.

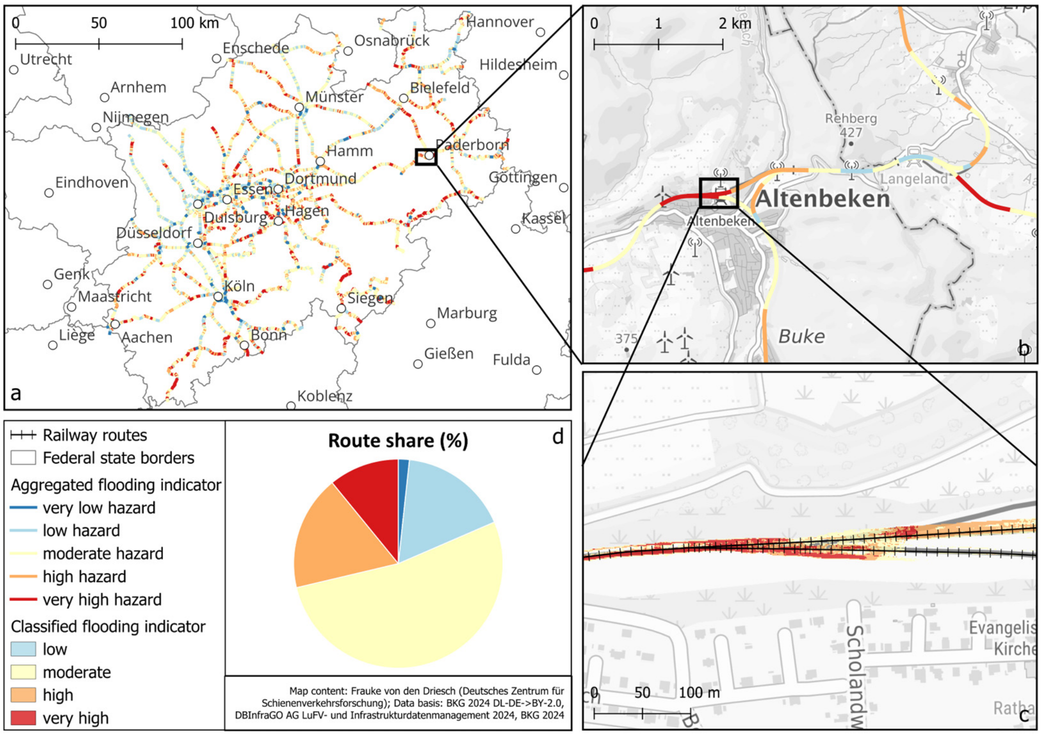

Figure 4. (**a**) Aggregated flooding indicator for potential exposure of the NRW railway network to an extreme heavy rainfall event (N_{ext}), (**b**) detailed view on vector-based aggregated flooding indicator, (**c**) detailed view on raster-based classified flooding indicator, and (**d**) proportions of route kilometres in the assigned aggregated flooding indicator classes.

The vector-based aggregated indicator in combination with the pixel-based result rasters within the buffered area can be used to gradually derive a multi-scale assessment of the heavy rainfall hazard for railway routes (Figure 4b,c). Thus, the results enable initial assessments of the impact at different scale levels. This means that hazard assessments can be derived at the network and route level using the aggregated flooding indicator, as well as on individual route segments, e.g., in the areas of railway stations.

The results of the aggregated flooding indicator for the heavy rainfall scenario N_{ext} for NRW are shown as an exemplary overview in Figure 4a. The static overview provides an initial indication and is not suitable for detailed analyses due to the spatial resolution, as not all railway lines can be visualised at this scale due to their spatial proximity. In the static overview maps, route sections with a higher hazard are visualised as a priority for technical reasons and can therefore overlay route sections with lower indicator classes. At this scale level, the higher indicator classes probably are visually exaggerated. The exact shares of the indicator classes in the route kilometres are shown in Figure 4d and described in Section 3.3. However, spatial analyses can rather be performed with the results as geodata and using flexible map views in GIS applications.

3.2. Regional Differentiation Analysis

In the regional differentiation analysis, spatial differences in the indicated heavy-rainfall hazards in the railway network in NRW for precipitation scenario N_{ext} (run A) were investigated in relation to the state's diverse topography. Approximately one third of the route kilometres in NRW are located in the relatively flat landscapes NBT (35%) and WFB (34%), a fifth in RSG (21%) and just under 10% in WBL, with the last two being characterised as low mountain ranges (Figure 5a).

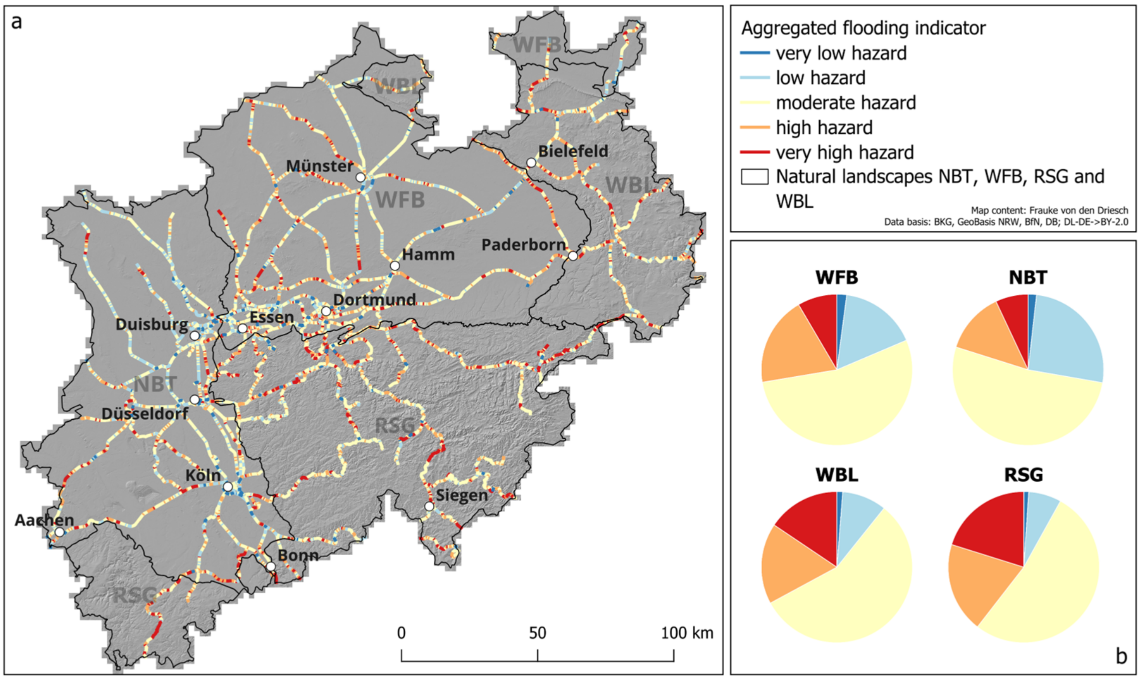

Figure 5. (**a**) Aggregated flooding indicator and (**b**) aggregated indicator class share for railway route kilometres in the landscapes Rheinisches Schiefergebirge (RSG), Niederrheinische Bucht und Tiefland (NBT), Weserbergland (WBL) and Westfälische Bucht (WFB) (N_{ext}).

In all landscapes, the proportion of route kilometres in the moderate hazard class is highest with around 50% (Figure 5b). The proportion of route kilometres with an indicated high or very high hazard of heavy rainfall is significantly greater in the low mountain regions RSG (39%) and WBL (40%) than in flat landscapes NBT (20%) and WFB (28%). This difference is specifically clear for very high hazard class shares with 7% (NBT) and 8% (WBT) for the flat landscapes in contrast to 20% (RSG) and 13% (WBL) for the mountainous landscapes. Consequently, the proportion of kilometres of routes with a low hazard of heavy rainfall is greater in the flat landscapes NBT (26%) and WFB (17%) than in the low mountain ranges RSG (7%) and WBL (9%). Very low hazard class shares are less than 2% in all four landscapes.

3.3. Scenario Analysis

In the scenario analysis, the aggregated hazard maps were analysed for the heavy-rainfall scenario N_{ext} (base run A) and the comparative scenario N_{100} (run B). First, the distribution of the aggregated flooding-indicator classes for both calculation runs A and B was examined to explore the reaction to different input scenarios. Therefore, the proportion of railway route kilometres in the five indicator classes was determined. The entire railway network in NRW comprises approximately 4800 km of routes. For both scenarios, the lowest proportion of kilometres is accounted for by the lowest indicator class very low hazard with ≤2% in each case (Figure 6a). The largest proportion of route kilometres in both calculation runs is in the moderate hazard indicator class with 53% (N_{ext}) and 54% (N_{100}). There are clear differences between the two calculation runs for the other classes. With 26%, the proportion of routes in the low hazard class in run B (N_{100}) is well above the proportion in the base run A (N_{ext}) (17%). In the high hazard and very high hazard indicator classes, the proportion of routes in run B (N_{100}) (12% and 6%) is clearly lower than in base run A (N_{ext}) (17% and 11%). The proportion in the class that represents the potentially highest hazard is therefore nearly twice as high in base run A (N_{ext}) as in run B (N_{100}). In both calculation runs, more than (N_{ext}) or nearly (N_{100}) two thirds of the kilometres of railway routes are classified as at least a moderate hazard. In base run A (N_{ext}), more than a quarter of the kilometres of railway routes are classified as high hazard or very high hazard, and nearly a fifth in run B (N_{100}).

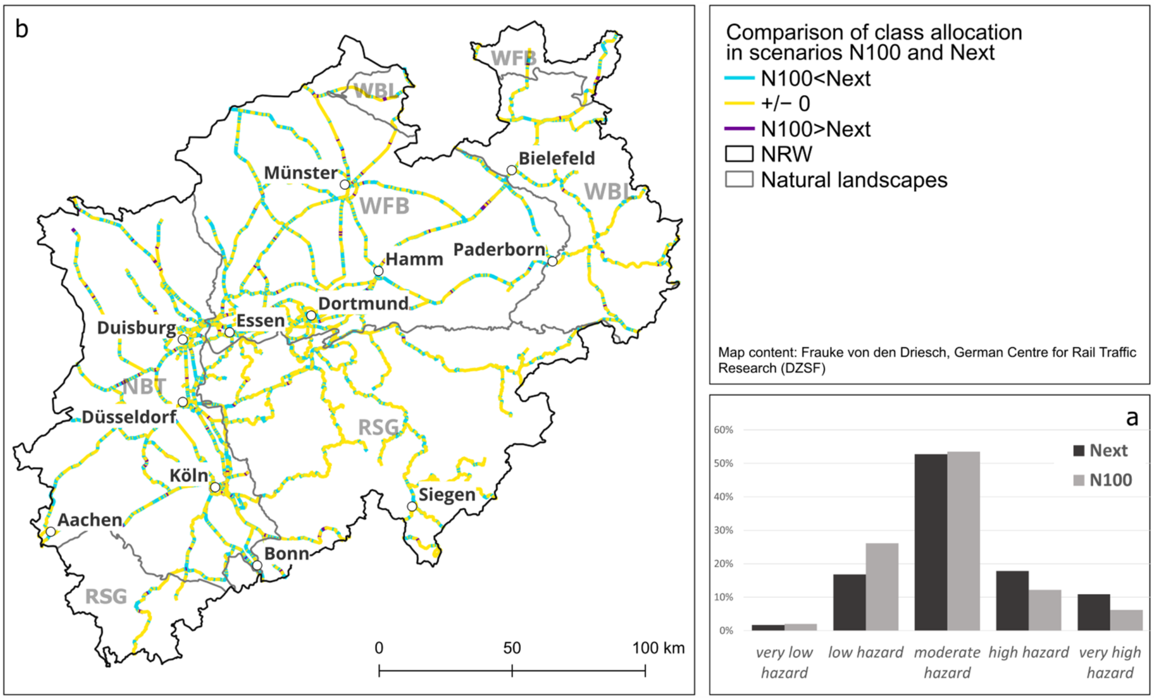

Figure 6. Comparison of resulting aggregated flooding indicator for base run A (scenario N_{ext}) and run B (scenario N_{100}) with (**a**) proportions of route kilometres in the aggregated indicator classes, and (**b**) spatial comparison of aggregated indicator class allocation.

Overall, the hazard class is the same for almost three quarters (72%) of the route kilometres in both calculation runs A and B (Figure 6b). Just under a quarter (24%) of route kilometres have a lower hazard class in run B (N_{100}) than in base run A (N_{ext}). Less than 2% of route kilometres are assigned a higher hazard class for run B (N_{100}) than in base run A (N_{ext}). Furthermore, in all landscapes, the proportion of route kilometres assigned the same hazard class in both calculation runs is greater than two thirds. The proportion of unchanged hazard classes is slightly higher in the low mountain ranges

(RSG 80%, WBL 78%) than in the flat landscapes (NBT 68%, WFB 70%). Subsequently, the proportion of route kilometres assigned a lower hazard class in run B (N_{100}) than in base run A (N_{ext}) is greater in flat landscapes (NBT 30%, WFB 26%) than in low mountain regions (RSG 18%, WBL 19%).

3.4. Structural Analysis

In the structural analysis, the relative influence of the classification decision for flooding depths on the resulting aggregated heavy rainfall indicator was explored by comparing the results of calculation run C with the results from base run A.

In run C more than two thirds (71%) of railway route kilometres are assigned the same flooding-indicator class as in base run A (Figure 7). Slightly less than a fifth (17%) of route kilometres are assigned a higher class and 12% are assigned a lower class in run C than in base run A. This pattern is similar across all four natural landscapes NBT, WFB, RSG and WBL. The majority of class transitions between base run A and run C happens within one level up or down. Nearly all of the class transitions from the *very low* and *low* classes between base run A and run C are into the next higher class. Most of the class transitions from high and very high hazard in base run A occur into the next lower hazard class, while a higher proportion from moderate class in base run A transitions to the next higher class than to the next lower class in run C.

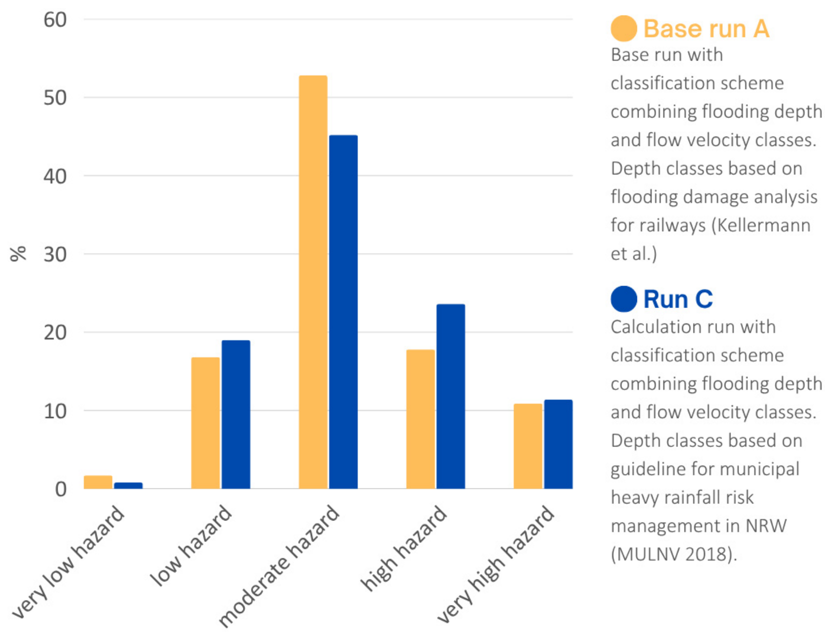

Figure 7. Proportions of route kilometres in the assigned aggregated flooding indicator classes for base run A and calculation run C in structural analysis [42,45].

3.5. Parameter Analysis

In the parameter analysis, the relative influence of the input parameters flooding depth and flow velocity on the resulting heavy rainfall hazards on the railway network was investigated. Therefore, the results of two additional runs with flooding depth (run D1) or flow velocity (run D2) as the sole input parameters were compared with a base run combining both parameters (base run C) to calculate the flooding indicator.

In run D1, three quarters (77%) of railway route kilometres were assigned the same aggregated flooding-indicator class as in base run C (Figure 8). Less than a fifth (17%) of route kilometres in run D1 are assigned a higher aggregated indicator class and 6% are assigned a lower indicator class than in the base run. This pattern is similar in all natural landscapes in NRW. Most of the class transitions between base run C and run D1 occur within one level up or down. Transitions from the *very low* and *low* classes between base run C and run D1 mostly occur to the next higher class. For the moderate, high and very high indicator classes, transitions to both the next lower and higher class occur between base run C and run D1.

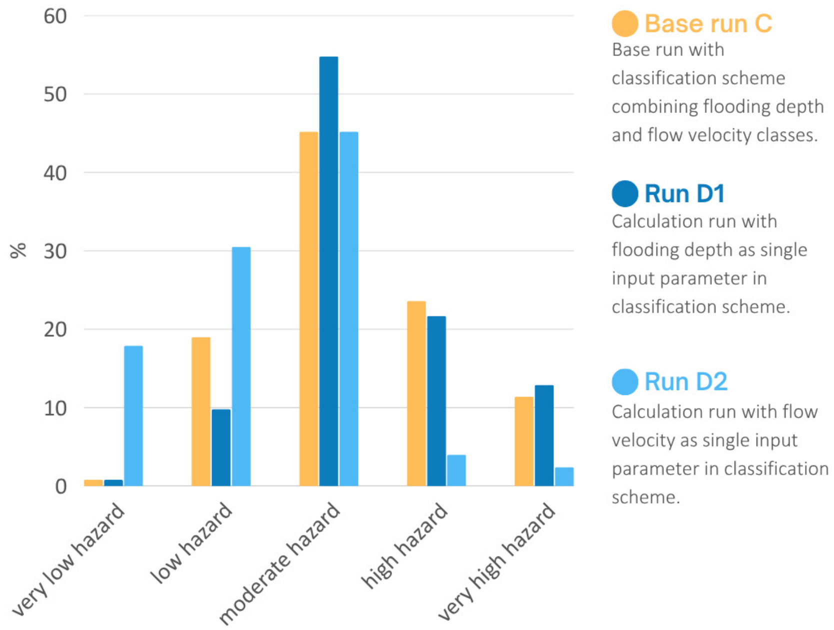

Figure 8. Proportions of route kilometres in the assigned aggregated flooding-indicator classes for base run C, calculation run D1 and calculation run D2 in parameter analysis.

In run D2, more than a third (35%) of railway route kilometres are assigned the same aggregated flooding-indicator class as in base run C (Figure 8). Nearly two thirds (64%) of route kilometres in run D2 are assigned a lower flooding-indicator class, while only one per cent is assigned a higher class in run D2 than in base run C. This pattern is similar in all natural landscapes in NRW. Most of the class transitions between base run C and run D2 occur within one or more levels down. Class transitions occur more likely for route sections assigned high or very high hazard than for the other classes.

3.6. Local Case Study: Railway Route 2631 Kall—Nettersheim During July 2021 Event

In the local case study, the plausibility of the resulting flooding-indicator was explored against a past heavy-rainfall event. Along the railway route section between Kall and Nettersheim, 5% of route kilometres were assigned low hazard, 49% moderate hazard, 14% high hazard and 32% very high hazard. There were no route segments assigned very low hazard in the route section under consideration (Figure 9). The three most frequent damage processes on the railway route 2631 between Kall and Nettersheim were mapped in a recent study: washout of ballast, gravel or soil; deposit of wood, branches or trees; and deposit of gravel or stone [11]. About half of the route section under consideration was affected by one or more of the mentioned damage processes. The mapped damage types occurred along the whole route section. On the one hand, damages occurred in route sections across all flooding indicator hazard classes. On the other hand, there are route sections in all hazard classes where none of the damage types considered here have been recorded.

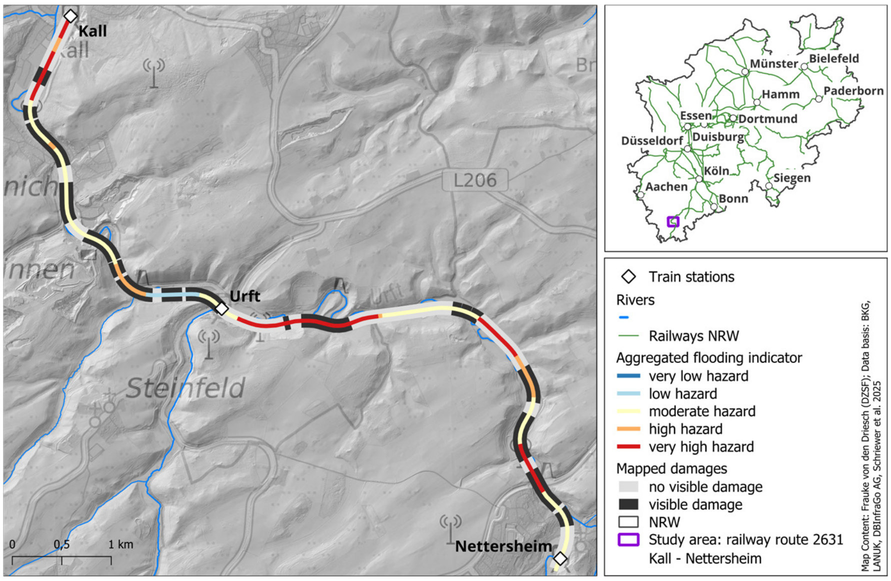

Figure 9. Aggregated flooding indicator (N_{ext}) and mapped selected types of damages [11] along railway route 2631 between the train stations Kall and Nettersheim.

4. Discussion

4.1. Development and Application of the Flooding Indicator

The flooding indicator developed provides a useful tool for initially identifying hazards in the railway network. The indicator was applied only for one federal state (NRW) so far, but as two of the most common regional landscapes in Germany, lowland regions and low mountain ranges, are present in NRW, similar results are expected for similar regions in Germany. By choosing a GIS-based approach with hazard indication maps as a product, a spatially explicit assessment of the heavy rainfall hazards was enabled. This approach is in line with other studies on climate hazards on railway networks [24–29] and complements the already available hazard indication maps at the German Centre for Rail Traffic Research (DZSF), which are used in research and practice [30].

The chosen rule-based classification and aggregation approach is based on parameters, classification schemes and thresholds established in the literature, which have already been empirically validated and/or applied in practice in the context of flooding hazard analyses [42,45,46,59]. The aim of this methodology is not to generate new empirical data, but rather to apply and adapt existing parameters, classification schemes and thresholds to the context of heavy rainfall and railway infrastructure. This approach ensures both the transparency and replicability of the results in context with existing studies and paves the way for its further development, implementation and application. In contrast to multi-criteria risk assessments [37–39], the flooding indicator presented here can be easily applied to the rest of the German railway network, developed further for scientific and practical questions or implemented in comprehensive risk analyses due to significantly less input data, which is already available for Germany, and a straight-forward workflow in open-source applications.

The parameters flooding depth and flow velocity were combined to derive a flooding indicator for heavy rainfall hazards on the railway network. On the one hand, considering both parameters influential for flooding hazards in general is in line with studies on flooding damages to railway infrastructure [11,42,44,53]. On the other hand, the approach is in contrast to multiple hazard studies related to flood impacts, which take flooding depth into account as the only or most important parameter for structural damage, focussing mostly on the less dynamic river flooding [42,43,59]. Still, multiple studies specifically emphasise the importance of flow velocity as a parameter in structural flood damage analyses for railway infrastructure, especially for flooding events with dynamic flow patterns, such as in the case of heavy-rainfall-induced flooding outside of running waters [37,42,53,59].

Despite this indication in the literature, no empirical classification scheme or threshold values for the damaging impacts of flow velocities specifically on railway infrastructure currently exists. To fill this gap, the developed flooding indicator used a rule-based approach from exposure and hazard analyses in municipal heavy rainfall risk management guidelines for the classification of flow velocity impacts on the railway network [45]. Originally developed for urban areas, the categorisation of hazards is based on the physical effect of water on structural components, such as doors and walls, and on associated processes. As the physical effects and processes, e.g., undermining, can be similar for railway infrastructure, the classification of flow velocities was assumed suitable in this study.

The classification of flooding depths was based on findings from river flooding damage analysis for railway infrastructure [42]. Heavy-rainfall-induced flooding and river flooding can lead to similar physical forces impacting infrastructure components. Both natural hazards can occur simultaneously, which also happened in July 2021 in Germany [10,11,61,62]. This makes it difficult to determine exactly which damage was caused by which process. The observed damages in a study of that event are generally more likely to be associated with river flooding than with heavy-rainfall-induced flooding outside the water body [11]. An empirical classification and threshold data especially for heavy-rainfall flooding damages is so far not available. Based on these findings, an empirical data basis on flooding depth related impacts of river flooding mechanisms was assumed suitable for the initial rule-based approach presented here [42]. This empirical data basis was already used for modelling estimated railway infrastructure damages and repair costs in Austrian Mur river catchment [59]. Still, heavy-rainfall events can lead to flooding with more dynamic and spatially diffuse flow patterns than river flooding, so empirical analyses of damages on railway infrastructure are needed to strengthen classification schemes and thresholds. In practice, however, conducting empirical studies is often difficult because detailed damage records for railway lines in Germany are maintained by the railway infrastructure companies, and this data is not generally made available for scientific studies. To address uncertainties, the assumption that damage can occur even in the lowest depth class was incorporated in the flooding indicator by introducing a fifth indicator class very low hazard. This assumption is in line with findings from current damage analysis on railway infrastructure [11].

However, the explorative parameter and structural analysis performed indicate the relative sensitivities and uncertainties of the literature-based methodology due to the lack of a broad empirical data basis. The results of both structural and parameter analysis are consistent across all natural landscapes in NRW, which underlines the general applicability of the approach to different topographies. The parameter analysis conducted showed that in this study the parameter flow velocity encourages a transition to lower flooding-indicator classes, while the parameter flooding depth encourages a transition to higher classes. Additionally, the variation of the classification scheme for flooding depth in the structural analyses emphasises that the resulting flooding indicator showed a relative sensitivity to the class boundaries. Based on that, a sensitivity to the class boundaries of flow velocity can also be assumed, even though there was no alternative classification scheme for flow velocity from the literature which could be used for comparison. Additionally, the parameter and structural analyses indicate that these relative sensitivities differ due to input parameter magnitude. These findings underline that more empirical basis is needed to strengthen classification schemes for flooding depth and flow velocity impact.

Consequently, additional flooding damage analyses of railway infrastructure relating to hydraulic parameters such as flooding depth, flow velocity and flow direction are needed to further develop flooding indicators as well as methodologies to perform detailed process analyses as well as adaptation studies.

The script-based and partially automated implementation of the approach in this study enables the reproducibility and replicability of the results, meaning that the approach can be applied to other input data technically and generate results that enable comparability. The use of Python as a scripting language in combination with QGIS functionalities as open-source tools enables easy implementation into existing systems and workflows. As the applications and scripting language used are available open source, they are also documented in a publicly accessible area. As Python and QGIS as well as GRASS GIS and SAGA GIS are constantly developed further, the workflow will need to be revised in relation to the modules, tools and their implementation. In principle, the methodology could also be applied using other scripting languages, e.g., R, and other GIS applications, e.g., ArcGIS. Additionally, the technical implementation promotes further scientific or practical development of the flooding-indicator as well as implementation in more comprehensive analysis. This is a major advantage compared to published railway damage studies [42,59] and multi-criteria assessments [37–39], which use complex models, algorithms and software applications, which are generally not freely available or are not specifically described. The flooding indicator methodology can thus easily be integrated into existing software structures from stakeholders and can be used there as an input parameter for further analyses, e.g., risk assessments.

The tile-by-tile processing of the input data and the cropping of the input data to an area of interest around the railway routes ensures a relatively low processing time. In this way, it is possible to produce results for large-scale investigation areas, e.g., entire federal states. In this processing method, there are forced splits at the tile boundaries dividing the railway route segments. Thus, constant segment lengths over the entire route network are not possible, resulting in track segments that are shorter than 500 m. This irregularity limits the comparability of the aggregated indicator in some places, as buffer areas of different sizes are taken into account in the aggregation.

4.2. Input Data

The derivation of the flooding indicator is based on the available modelled flooding depths and flow velocities. These parameters were generated in a project to derive Germany-wide heavy-rainfall hazard indication maps aiming at complete coverage and thus an information function at an overview level [40,41]. In a river-flood damage analysis on railways, hydraulic modelling was used to derive hydraulic parameters, e.g., flooding depth and flow velocity [42]. In contrast, multi-criteria assessment studies on flooding hazards to railways did not perform hydraulic or hydrological modelling with high-resolution input data, but rather produced hydrological information from lower resolution geo data using terrain-analysis tools in GIS [37,39]. This information is less accurate than the 2D-modelled data used in our investigation.

The vector data set of the railway network used for the analysis contains the routes as polylines, but not the exact track position. As there are single-track and double-track routes in the German railway network, the position of the polylines in the dataset deviates spatially from the actual track position to varying degrees. To address this uncertainty in the data, the flooding indicator was derived from flooding depths and flow velocities in a 10 m buffer area around the routes. Consequently, it is assumed that the tracks are in this area as well as other threatened infrastructural components, e.g., signals or power supply. Therefore, the input data with inaccurate track positions can be considered sufficient here, as the methodology provides results at an indicative level. On the other hand, the exact topographical location of tracks and other infrastructure components, e.g., on a dam or along an embankment, and its associated influence on local flooding patterns, cannot be depicted using the flooding indicator presented here. For specific infrastructure planning, further high-resolution analyses, as well as more detailed input data, are necessary, e.g., on the exact position of infrastructure assets, local soil properties or diverse precipitation scenarios. The flooding indicator presented here can serve as a starting point for these local processes.

4.3. Indicated Heavy Rainfall Hazards in NRW

The results of the study could not be verified against historical events as there was no suitable comprehensive damage data available at the time the study was conducted. However, the study area includes parts of the railway network that were affected by the extreme flooding event in July 2021. A local case study performed with limited damage data showed that damages occurred along the whole route section and in all hazard classes. For the whole route section, a relatively high exposure to heavy rainfall impacts can be considered, as 95% of the route section were assigned at least moderate hazard with more than a third of route kilometres being assigned very high hazard. The indicated hazard corresponded to the mapped damages, which strengthened the plausibility of the flooding-indicator approach and its results. Nevertheless, there is no validation possible based on the available data. The July 2021 event was so severe that damages occurred across the entire region [8,10,11,14,19], flooding from the Urft river affected the infrastructure as well [11], and the local case study railway route section is very short (<10 km) in relation to the whole network in NRW. Additionally, the underlying geodata was not available, which increased the inaccuracy of the analysis conducted. However, the local case study showed that the flooding-indicator results are in general suitable for comparison with actual flood damage from past events. Such analyses with historical damage data are needed to develop the approach further as well as to perform local risk analyses of railways. Given the dynamic of the July 2021 heavy rainfall and flooding event, combined analysis of river flooding and heavy rainfall hazards at regional and local levels should be considered for flooding impacts on the railway network.

The regional differentiation analysis has already revealed spatial patterns of potential heavy-rainfall hazards to the railway network in NRW. The characteristics of the flooding indicator in low mountain ranges and lowland regions, as well as the differences between them, could provide indications of the potential heavy-rainfall hazards to railway infrastructure in similar landscapes in Germany. These regional patterns are in line with studies identifying steeper slope as promoting factor for flash floods, e.g., [63–66] and high flooding hazards in mountain areas, e.g., [63,66,67], and they strengthen the plausibility and spatial transferability of the flooding indicator results. Additionally, this pattern fit with the local case study, which showed high hazard and corresponding historical flooding damages along a railway route in the Eifel low mountain range.

The scenario analysis conducted showed a general tendency towards a lower hazard classification for the N_{100} scenario compared to the N_{ext} scenario, which is plausible considering the lower precipitation intensity of N_{100} scenario. These findings are in line with studies on the severity of heavy-rainfall-induced flooding related to precipitation frequencies and durations, e.g., [68,69]. Additionally, the differences between the 100-year scenario and the extreme scenario are greater in the flat regions than in the low mountain regions. These relative sensitivities showed the relevance of considering multiple precipitation scenarios to strengthen the informative value of the flooding indicator in further local studies or practical questions. As the equivalent comprehensive data are not

https://doi.org/10.3390/w18131533

yet available, no other precipitation scenarios were examined. With regard to the further development and practical applicability of the flooding indicator, it would be useful to investigate scenarios of lower intensities than N_{100} and N_{ext}. However, the methodology presented here offers flexibility with regard to input scenarios and can therefore contribute to addressing more detailed and local issues.

Hazard indication maps generally allow an initial assessment of the exposure of the transport infrastructure to the climate impact—in this case, heavy rainfall [70]. In this sense, a statement cannot be made about the actual impact on the railway infrastructure in the event of heavy rainfall based on either the data basis or the flooding indicator. The aim of this study is to provide a tool for the qualitative and classified assessment of heavy rainfall hazards. Thus, with the derivation of the flooding indicator, the inaccuracies and uncertainties of the underlying modelling were taken into account. The derivation of a classified and an aggregated indicator enables intuitive grasping of the hazard assessment and is therefore suitable for practical application in the railway sector while not requiring detailed knowledge of heavy rainfall processes and modelling. The results of this study can therefore serve as starting points for further analyses, e.g., climate impact analyses or risk analyses for heavy rainfall. Further climate impact analyses and risk assessments can contribute to deriving localised need for action with regard to adapting the railway network to heavy rainfall events [30,70].

Neither the underlying modelled flooding depths and flow velocities nor the derived flooding indicator are suitable for quantitative statements at a detailed level, as would be necessary, for example, for the specific planning of adaptation measures. Multiple other parameters, e.g., for the criticality and sensitivity of infrastructure assets such as drainage systems, should be taken into account to drive forward more detailed adaptation planning [36,37]. The flooding indicator provides a valid starting point for these detailed analyses, thus creating a basis and a first step for increasing the resilience of railway networks to heavy rainfall hazards.

5. Conclusions

This study makes an important contribution to increasing the resilience of the German railway network to heavy rainfall hazards. An initial approach for assessing the exposure and hazard of heavy rainfall to the railway infrastructure was developed and applied to the railway network in NRW. The research questions were addressed by developing a rule-based classification approach, visualising the flooding indicator as hazard indication maps and assessing the resulting indicated heavy rainfall hazards for NRW. The methodology developed is in line with the study's objective to provide an easily replicable tool for indicative exposure and hazard analyses in the German railway network using already available high-quality data. The study has shown that in both of the precipitation scenarios considered, N_{100} and N_{ext}, the clear majority of the route kilometres in the study area are classified as being at least moderate hazard. Considering the expected increase in extreme events in the course of climate change, the results thus show the necessity of adapting the railway infrastructure to heavy rainfall impacts.

The maps produced serve as an exposure analysis as part of a climate impact analysis of heavy rainfall hazards to the German railway network. Furthermore, the maps can serve as a starting point for making qualitative statements on the potential impact on the railway network and localising these impacts spatially. The results of this study cannot provide a quantitative statement on the actual impact of heavy rainfall on the German railway network. They could not be validated with recordings of current heavy rainfall events due to the lack of suitable and sufficient data. However, a local comparison with exemplary damage points from the July 2021 flooding event generally showed consistency between the indicated hazards and route sections affected. With regard to the data basis available in the future as well as practical questions in infrastructure planning, the aim should be to further develop the methodology by incorporating more comprehensive empirical data and parameters, and to extend the flooding-indicator maps to the whole of Germany. Hence, future scientific and practical questions could explore the economic and operational implications of heavy rainfall hazards and could use additional data, e.g., on other precipitation scenarios, higher-resolution data of infrastructure assets as well as damage costs.

Especially against the background of recent heavy rainfall events, this study should serve as an impetus to locate hot spots of potential heavy rainfall impact in the railway network and to carry out detailed analyses with regard to adaptation options. The development of an adaptation strategy including a catalogue of measures that includes technical, structural and/or regulatory adaptation measures, for example, would greatly contribute to the climate adaptation of the German railway network.

Author Contributions: Conceptualization, F.v.d.D.; Methodology, F.v.d.D.; Software, F.v.d.D.; Validation, F.v.d.D.; Formal Analysis, F.v.d.D.; Investigation, F.v.d.D.; Resources, F.v.d.D.; Data Curation, F.v.d.D.; Writing—Original Draft Preparation, F.v.d.D.; Writing—Review and Editing, F.v.d.D. and S.S.; Visualisation, F.v.d.D.; Project Administration, F.v.d.D. All authors have read and agreed to the published version of the manuscript.

Funding: This research was carried out in the topic area "Climate Change Impacts and Adaptation" of the BMV Research Network, a cross-modal research format in the BMV's departmental research. Research work in this network is funded by the German Federal Ministry for Transport (BMV).

Data Availability Statement: The input data was derived from the following resources available in the public domain: (a) heavy rainfall indication maps NRW at [41], (b) Deutsche Bahn railway network at [49]. Damage data for the local case study was derived from the publication at [11]. The processing code and the resulting datasets presented in this article are not readily available because the data are part of an ongoing study. Requests to access the resulting datasets should be directed to vondendrieschf@dzsf.bund.de.

Acknowledgments: The authors would like to thank the members of the BMV Research Network, topic area "Climate Change Impacts and Adaptation", for fruitful discussions.

Conflicts of Interest: The authors declare no conflicts of interest.

References

1. Ludvigsen, J.; Klaeboe, R. Extreme weather impacts on freight railways in Europe. *Nat. Hazards* **2013**, *70*, 767–787. [CrossRef]
2. Gössling, S.; Neger, C.; Steiger, R.; Bell, R. Weather, climate change, and transport: A review. *Nat. Hazards* **2023**, *118*, 1341–1360. [CrossRef]
3. Palin, E.; Oslakovich, I.; Gavin, K.; Quinn, A. Implications of climate change for railway infrastructure. *WIREs Clim. Change* **2021**, *12*, e728. [CrossRef]
4. Destatis. *Schieneninfrastruktur: Betriebsstreckenlänge Nach Bundesländern*; Destatis: Wiesbaden, Germany, 2023. Available online: https://www.destatis.de/DE/Themen/Branchen-Unternehmen/Transport-Verkehr/Unternehmen-Infrastruktur-Fahrzeugbestand/Tabellen/schieneninfrastruktur.html (accessed on 12 September 2025).
5. Eurostat. *Beförderte Fahrgäste Nach Beförderungsart (Ausführliche Berichterstattung)*; Eurostat: Luxembourg, 2025. Available online: https://ec.europa.eu/eurostat/databrowser/view/rail_pa_typepas/default/table?lang=de (accessed on 12 September 2025).
6. Eurostat. *Beförderte Güter Nach Beförderungsart (Ausführliche Berichterstattung)*; Eurostat: Luxembourg, 2025. Available online: https://ec.europa.eu/eurostat/databrowser/view/rail_go_typepas/default/table?lang=de (accessed on 12 September 2025).
7. Fabella, V.; Szymczak, S. Resilience of railway transport to four types of natural hazards: An analysis of daily train volumes. *Infrastructures* **2021**, *6*, 174. [CrossRef]
8. Koks, E.; van Ginkel, K.; van Maarle, M.; Lemnitzer, A. Brief communication: Critical infrastructure impacts of the 2021 mid-July western European flood event. *Nat. Hazards Earth Syst. Sci.* **2022**, *22*, 3831–3838. [CrossRef]

9. Szymczak, S.; Bott, F.; Fabella, V.M.; Fricke, K. Are heavy rainfall events a major trigger of associated natural hazards along the German rail network? *Nat. Hazards Earth Syst. Sci.* **2025**, *25*, 683–707. [CrossRef]
10. Szymczak, S.; Backendorf, F.; Bott, F.; Fricke, K.; Junghänel, T.; Walawender, E. Impacts of heavy and persistent precipitation on railroad infrastructure in July 2021: A case study from the Ahr Valley, Rhineland-Palatinate, Germany. *Atmosphere* **2022**, *13*, 1118. [CrossRef]
11. Schriewer, E.-L.; Hofmann, J.; Stenger-Wolf, S.; Szymczak, S.; Vaitl, T.; Schüttrumpf, H. Damage analysis of the Eifel route railroad infrastructure after the flash flood event in July 2021 in western Germany. *Water* **2025**, *17*, 2874. [CrossRef]
12. DeVinne, N.; DeBold, R.; Forde, M.; Ho, C. Impact of climate change on railway construction, maintenance and safety in the United Kingdom. In *Proceedings of the 11th International Conference on the Bearing Capacity of Roads, Railways and Airfields (BCRRA)*; Hoof, M., Mork, H., Saba, M., Eds.; CRC Press: Boca Raton, FL, USA, 2022; Volume 2.
13. Deutsche Bahn AG. *Auf Über 85% der vom Wasser Zerstörten Infrastruktur Fahren Heute Wieder Züge*; Deutsche Bahn AG: Berlin, Germany, 2022. Available online: https://www.deutschebahn.com/de/presse/presse-regional/pr-frankfurt-de/presseinformationen-regional/auf-ueber-85-prozent-der-vom-wasser-zerstoerten-infrastruktur-fahren-heute-wieder-zuege--8853616# (accessed on 16 January 2025).
14. DB InfraGo AG. *Antworten Auf Die Häufigsten Fragen Zum Wiederaufbau Nach der Flutkatastrophe Und Zur Elektrifizierung*; DB InfraGo AG: Frankfurt am Main, Germany, 2025. Available online: https://flut-aufbau.deutschebahn.com/ (accessed on 21 November 2025).
15. Spekkers, M.; Rözer, V.; Thieken, A.; ten Veldhuis, M.; Kreibich, H. A comparative survey of the impacts of extreme rainfall in two international case studies. *Nat. Hazards Earth Syst. Sci.* **2017**, *17*, 1337–1355. [CrossRef]
16. Walter, D. Fast Ein Jahr Nach Dem Starkregen: An Wichtiger ICE-Trasse Wird Immer Noch Gebaut. Merkur. 2025. Available online: https://www.merkur.de/bayern/nuernberg/nuernberg-wuerzburg-kitzingen-wochen-lang-gesperrt-hochwasser-bauarbeiten-bahnstrecke-93121507.html (accessed on 21 November 2025).
17. Handelsblatt. Hochwasser in Süddeutschland: ICE entgleist bei Schwäbisch Gmünd. 2024. Available online: https://www.handelsblatt.com/politik/deutschland/hochwasser-in-sueddeutschland-ice-entgleist-bei-schwaebisch-gmuend/100042047.html (accessed on 11 June 2026).
18. Dietze, M.; Bell, R.; Ozturk, U.; Cook, K.; Andermann, C.; Beer, A.; Damm, B.; Lucia, A.; Fauer, F.; Nissen, K.; et al. More than heavy rain turning into fast-flowing water—A landscape perspective on the 2021 Eifel floods. *Nat. Hazards Earth Syst. Sci.* **2022**, *22*, 1845–1856. [CrossRef]
19. Dunkerley, D. Rainfall intensity in geomorphology: Challenges and opportunities. *Prog. Phys. Geogr. Earth Environ.* **2020**, *45*, 3–26. [CrossRef]
20. Brasseur, G.; Jacob, D.; Schuck-Zöller, S. *Klimawandel in Deutschland: Entwicklung, Folgen, Risiken und Perspektiven*; Springer Spektrum: Berlin/Heidelberg, Germany, 2023.
21. Ortega, E.; Martín, B.; Aparicio, Á. Identification of critical sections of the Spanish transport system due to climate scenarios. *J. Transp. Geogr.* **2020**, *84*, 102690. [CrossRef]
22. Wu, Y.; Hayat, T.; Clarens, A.; Smith, B. Climate change effects on transportation infrastructure—Scenario-based risk analysis using geographic information systems. *Transp. Res. Rec.* **2013**, *2375*, 71–81. [CrossRef]
23. Hawchar, L.; Naughton, O.; Nolan, P.; Stewart, M.; Ryan, P. A GIS-based framework for high-level climate change risk assessment of critical infrastructure. *Clim. Risk Manag.* **2020**, *29*, 100196. [CrossRef]
24. Bíl, M.; Andrásik, R.; Nezval, V.; Bílová, M. Identifying locations along railway networks with the highest tree fall hazard. *Appl. Geogr.* **2017**, *87*, 45–53. [CrossRef]
25. Arango, E.; Jiménez, P.; Nogal, M.; Sousa, H.S.; Stewart, M.G.; Matos, J.C. Enhancing infrastructure resilience in wildfire management to face extreme events: Insights from the Iberian Peninsula. *Clim. Risk Manag.* **2024**, *44*, 100595. [CrossRef]
26. Meine, L.; Lohrengel, A.-F. Überflutungen Durch Starkregen: Blue-Spot-Analyse für das Fernstraßennetz in NRW. Forschungsergebnisse Kompakt. 2021. Available online: https://www.bmv-forschungsnetzwerk.bund.de/de/publikationen/kurzberichte/tf1/meine_2021.pdf?__blob=publicationfile&v=2 (accessed on 30 January 2025).
27. Büche, K.; Assmann, H.; Huber, B.; Henrichs, T.; Pulgrabja, J. *Lokale Analyse und Kartierung von potenziellen Überflutungsflächen im Bundesfernstraßennetz von Nordrhein-Westfalen in Folge von Starkregenereignissen (Blue-Spot-Analyse)*; Berichte der Bundesanstalt für Straßen- und Verkehrswesen Straßenbau, Heft S 231; Fachverlag NW in der Carl Ed. Schünemann KG: Bremen, Germany, 2026. [CrossRef]
28. Rinderer, M.; Berger, C.; Zimmermann, F.; Mertin, M.; Jäger, S. Analysen zu schnellen wasserhaltigen Massenbewegungen. Bundesweite Untersuchungen zur Exposition des deutschen Schienennetzes und Modellierungen der räumlichen Ausbreitung. *Berichte Dtsch. Zent. Schienenverk.* **2023**, *48*, 115. [CrossRef]
29. Frick, A.; Wagner, K.; Stöckigt, B. Sensitivitätsanalyse Vegetation entlang der Bundesverkehrswege bezüglich Sturmwurfgefahren und Böschungsbränden. *Berichte Dtsch. Zent. Schienenverk.* **2023**, *41*, 127. [CrossRef]

30. Szymczak, S.; Bott, F.; von den Driesch, F. Gefahrenhinweiskarten als Tool der Klimafolgenanpassung im Schienenverkehr. *gis. Science* **2025**, *1*, 1–12. [CrossRef]
31. Ochsner, M.; Palmqvist, C.; Olsson, N.; Winslott Hiselius, L. The effects of flooding on railway infrastructure: A literature review. *Transp. Res. Procedia* **2023**, *72*, 1786–1791. [CrossRef]
32. Cheetham, M.; Tourment, R.; Pelt, P. Risk assessment and economic appraisal of protection methods for the Tarascon–Arles railway embankment. *E3S Web Conf.* **2016**, *7*, 11005. [CrossRef]
33. Murphy, A.; Gouldby, B.; Cole, S.; Moore, R.; Kendall, H. Real-time flood inundation forecasting and mapping for key railway infrastructure: A UK case study. *E3S Web Conf.* **2016**, *7*, 11006. [CrossRef]
34. Pregnolato, M.; Dawson, D. Adaptation investments for transport resilience: Trends and recommendations. *Int. J. Saf. Secur. Eng.* **2018**, *8*, 515–527. [CrossRef]
35. Hong, L.; Ouyang, M.; Peeta, S.; He, X.; Yan, Y. Vulnerability assessment and mitigation for the Chinese railway system under floods. *Reliab. Eng. Syst. Saf.* **2015**, *137*, 58–68. [CrossRef]
36. Liu, K.; Wang, M.; Cao, Y.; Zhu, W.; Yang, G. Susceptibility of existing and planned Chinese railway systems subjected to rainfall-induced multi-hazards. *Transp. Res. Part A* **2018**, *117*, 214–226. [CrossRef]
37. Oliveira de Sousa, F.; Ariza Flores, V.; Cunha, C.; Oda, S.; Xavier Ratton Neto, H. Multi-criteria assessment of flood risk on railroads using a machine learning approach: A case study of railroads in Minas Gerais. *Infrastructures* **2025**, *10*, 12. [CrossRef]
38. Apollonio, C.; Iemmolo, G.; Di Modugno, M.; Apollonio, M.; Petroselli, A.; Recanatesi, F.; Giannetta, D. A Multi-Parameter Approach to Support Sustainable Hydraulic Risk Analysis for the Protection of Transportation Infrastructure: The Case Study of the Gargano Railways (Southern Italy). *Sustainability* **2025**, *17*, 4151. [CrossRef]
39. Chaulagain, D.; Rimal, P.; Ngando, S.; Kigha Nsafon, B.; Suh, D.; Huh, J. Flood susceptibility mapping of Kathmandu metropolitan city using GIS-based multi-criteria decision analysis. *Ecol. Indic.* **2023**, *154*, 110653. [CrossRef]
40. Bundesamt für Kartographie und Geodäsie (BKG). *Erfolgreicher Auftakt: Bundesweite Kartierung Über Die Gefahren Durch Starkregen Gestartet*; BKG: Frankfurt am Main, Germany, 2023. Available online: https://www.bkg.bund.de/shareddocs/pressemitteilungen/bkg/de/pm_2023/230511-kickoff-starkregen.html (accessed on 17 January 2025).
41. Bundesamt für Kartographie und Geodäsie (BKG). *WMS Hinweiskarte Starkregengefahren*; BKG: Frankfurt am Main, Germany, 2024. Available online: https://gdz.bkg.bund.de/index.php/default/wms-hinweiskarte-starkregengefahren-wms-starkregen.html (accessed on 17 January 2025).
42. Kellermann, P.; Schöberl, A.; Kundela, G.; Thieken, A. Estimating flood damage to railway infrastructure—The case study of the March River flood in 2006 at the Austrian Northern Railway. *Nat. Hazards Earth Syst. Sci.* **2015**, *15*, 2485–2496. [CrossRef]
43. Zhu, W.; Liu, K.; Ming, W.; Ward, P.; Koks, E. System vulnerability to flood events and risk assessment of railway systems based on national and river basin scales in China. *Nat. Hazards Earth Syst. Sci.* **2022**, *22*, 1519–1540. [CrossRef]
44. Tsubaki, R.; Bricker, J.; Ichii, K.; Kawahara, Y. Development of fragility curves for railway embankment and ballast scour due to overtopping flood flow. *Nat. Hazards Earth Syst. Sci.* **2016**, *16*, 2455–2472. [CrossRef]
45. Ministerium für Umwelt. Landwirtschaft, Natur- Und Verbraucherschutz des Landes Nordrhein-Westfalen (MULNV NRW). In *Arbeitshilfe Kommunales Starkregenrisikomanagement*; MULNV NRW: Düsseldorf, Germany, 2018.
46. Landesanstalt für Umwelt Baden-Württemberg (LUBW). *Kommunales Starkregenrisikomanagement in Baden-Württemberg*; LUBW: Karlsruhe, Germany, 2016.
47. DB InfraGo. Europäische Güterverkehrskorridore (SGV-Korridore). Available online: https://www.dbinfrago.com/ (accessed on 26 November 2025).
48. Deutscher Bundestag. *Antwort der Bundesregierung auf Die Kleine Anfrage der Abgeordneten Torsten Herbst, Frank Sitta, Dr. Christian Jung, Weiterer Abgeordneter Und der Fraktion der FDP—Drucksache 19/19475—Verlässlichkeit des Schienenverkehrs an Knotenbahnhöfen*; Deutscher Bundestag: Berlin, Germany, 2020. Available online: https://dserver.bundestag.de/btd/19/204/1920455.pdf (accessed on 25 November 2025).
49. Deutsche Bahn AG. *Infrastrukturdaten der DB InfraGo AG*; Deutsche Bahn AG: Berlin, Germany, 2025. Available online: https://mobilithek.info/offers/922109165921083392 (accessed on 10 January 2025).
50. Schmitt, T.G. Starkregenindex zur Kommunikation von Überflutungsursachen und Risiken. *KA Korresp. Abwasser Abfall* **2014**, *61*, 681–687. [CrossRef]
51. Schmitt, T.G. Weiterentwicklung des Starkregenindex zur Verwendung in der kommunalen Überflutungsvorsorge. *gwf-Wasser/Abwasser* **2015**, *156*, 774–781.
52. Nikogosian, C.; Winterrath, T.; Walawander, E.; Fischer, I.; Schmitz-Kröll, D.; Wischott, V. Klassifikation meteorologischer Extremereignisse zur Risikovorsorge gegenüber Starkregen für den Bevölkerungsschutz und die Stadtentwicklung. Projekt der Strategischen Behördenallianz "Anpassung an den Klimawandel". *Abschlussbericht* 2021. Available online: https://www.bbk.bund.de/SharedDocs/Downloads/DE/Mediathek/Publikationen/Klimawandel/klamex-abschlussbericht.pdf?__blob=publicationFile&v=7 (accessed on 28 November 2025).

53. Kreibich, H.; Piroth, K.; Seifert, I.; Maiwald, H.; Kunert, U.; Schwarz, J.; Merz, B.; Thieken, A. Flood damage analysis—Results from Germany. *Nat. Hazards Earth Syst. Sci.* **2009**, *9*, 1679–1692. [CrossRef]
54. Vanneuville, W.; De Maeyer, P.; Koen, M.; Mostaert, F. Model of the effects of a flood in the Dender catchment, based on a risk methodology. *Bull. Soc. Cartogr.* **2003**, *37*, 59–64.
55. Kok, M.; Huizinga, H.; Vrouwenvelder, A.; Barendregt, A. *Standard Method 2004: Damage and Casualties Caused by Flooding*; Rijkswaterstaat: Delft, The Netherlands, 2004.
56. Deckers, P.; Kellens, W.; Reyns, J.; Vanneuville, W.; De Maeyer, P. A GIS for flood risk management in Flanders. In *Geospatial Techniques in Urban Hazard and Disaster Analysis*; Showalter, P., Lu, Y., Eds.; Springer: Dordrecht, The Netherlands, 2010; pp. 51–66.
57. Martello, M.; Whittle, A.; Lyons-Galante, H. Depth-damage curves for rail rapid transit infrastructure. *J. Flood Risk Manag.* **2023**, *16*, e12853. [CrossRef]
58. Murdock, H.; de Bruijn, K.; Gersonius, B. Assessment of critical infrastructure resilience to flooding using a response curve approach. *Sustainability* **2018**, *10*, 3470. [CrossRef]
59. Kellermann, P.; Schönberger, C.; Thieken, A. Large-scale application of the flood damage model Railway Infrastructure Loss (RAIL). *Nat. Hazards Earth Syst. Sci.* **2016**, *16*, 2357–2371. [CrossRef]
60. Geologischer Dienst NRW. Naturräume in NRW. Available online: https://www.gd.nrw.de/ge_ev_naturraeume-nrw.htm (accessed on 28 November 2025).
61. Junghänel, T.; Bissolli, P.; Daßler, J.; Fleckenstein, R.; Imbery, F.; Janssen, W.; Kaspar, F.; Lengfeld, K.; Leppelt, T.; Rauthe, M.; et al. *Hydro-Klimatologische Einordnung der Stark- Und Dauerniederschläge in Teilen Deutschlands im Zusammenhang Mit Dem Tiefdruckgebiet "Bernd" Vom 12. Bis 19. Juli 2021*; Deutscher Wetterdienst: Offenbach am Main, Germany, 2021. Available online: https://www.dwd.de/DE/leistungen/besondereereignisse/niederschlag/20210721_bericht_starkniederschlaege_tief_bernd.pdf (accessed on 20 March 2026).
62. Bund/Länder-Arbeitsgemeinschaft Wasser (LAWA). Analyse Zum Juli-Hochwasser 2021 und Ableitung von Konsequenzen aus Sicht des LAWA-AH. Deutschland, 2022. Available online: https://www.lawa.de/documents/analyse-zum-juli-hochwasser-2021-barrierefrei_1689857053.pdf (accessed on 20 March 2026).
63. Víg, B.; Fábian, S.Á.; Czigány, S.; Pirkhoffer, E.; Halmai, Á.; Kovács, I.P.; Varga, G.; Dezső, J.; Nagy, G.; Lóczy, D. Morphometric analysis of low mountains for mapping flash flood susceptibility in headwaters. *Nat. Hazards* **2022**, *114*, 3235–3254. [CrossRef]
64. Abdo, H.G. Evolving a total-evaluation map of flash flood hazard for hydro-prioritization based on geohydromorphometric parameters and GIS–RS manner in Al-Hussain river basin, Tartous, Syria. *Nat. Hazards* **2020**, *104*, 681–703. [CrossRef]
65. Douinot, A.; Iffly, J.F.; Tailliez, C.; Meisch, C.; Pfister, L. Flood patterns in a catchment with mixed bedrock geology and a hilly landscape: Identification of flashy runoff contributions during storm events. *Hydrol. Earth Syst. Sci.* **2022**, *26*, 5185–5206. [CrossRef]
66. Brázdil, R.; Faturová, D.; Šulc Michalková, M.; Řehoř, J.; Caletka, M.; Zahradníček, P. Spatiotemporal variability of flash floods and their human impacts in the Czech Republic during the 2001–2023 period. *Nat. Hazards Earth Syst. Sci.* **2024**, *24*, 3663–3682. [CrossRef]
67. Kaiser, M.; Borga, M.; Disse, M. Occurrence and Characteristics of Flash Floods in Bavaria (Germany). In *Climate Change Management*; Springer: Cham, Switzerland, 2020; pp. 293–310. [CrossRef]
68. Li, Z.; Gao, S.; Chen, M.; Zhang, J.; Gourley, J.J.; Wen, Y.; Yang, T.; Hong, Y. Introducing Flashiness-Intensity-Duration-Frequency (F-IDF): A New Metric to Quantify Flash Flood Intensity. *Geophys. Res. Lett.* **2023**, *50*, e2023GL104992. [CrossRef]
69. Saharia, M.; Kirstetter, P.-E.; Vergara, H.; Gourley, J.J.; Emmanuel, I.; Andrieu, H. On the Impact of Rainfall Spatial Variability, Geomorphology, and Climatology on Flash Floods. *Water Resour. Res.* **2021**, *57*, e2020WR029124. [CrossRef]
70. Hänsel, S.; Hillebrand, G.; Nilson, E.; Rauthe, M.; Lohrengel, A.-F.; Meine, L.; Herrmann, C.; Brendel, C.; Forbriger, M.; Kirsten, J.; et al. *Klimawirkungsanalyse für Die Bundesverkehrswege—Methodik und Erste Ergebnisse. Schlussbericht*; BMVI-Expertennetzwerk: Berlin, Germany, 2020. [CrossRef]

https://doi.org/10.3390/w18131533